AD-A032 680 NAVAL RESEARCH LAB WASHINGTON D C F/G 4/1
NONSTEADY LABORATORY SIMULATION OF ATMOSPHERIC VORTICES: INERTI--ETC(U)
OCT 76 J A KAISER

UNCLASSIFIED NRL-8046 NL

| OF |
AD
A032680

END

DATE
FILMED
1-77

NRL Report 8046

12

Nonsteady Laboratory Simulation of Atmospheric Vortices: Inertial Oscillations and Tornado Skip

JACK A. C. KAISER

Physical Oceanography Branch
Ocean Sciences Division

October 13, 1976

NAVAL RESEARCH LABORATORY
Washington, D.C.

SECURITY CLASSIFICATION OF THIS PAGE *(When Data Entered)*

REPORT DOCUMENTATION PAGE

READ INSTRUCTIONS BEFORE COMPLETING FORM

1. REPORT NUMBER
NRL Report 8046

2. GOVT ACCESSION NO.

3. RECIPIENT'S CATALOG NUMBER

4. TITLE *(and Subtitle)*
Nonsteady Laboratory Simulation of Atmospheric Vortices: Inertial Oscillations and Tornado Skip

5. TYPE OF REPORT & PERIOD COVERED
Interim report on a continuing NRL Problem

6. PERFORMING ORG. REPORT NUMBER

7. AUTHOR(s)
Jack A.C. Kaiser

8. CONTRACT OR GRANT NUMBER(s)

9. PERFORMING ORGANIZATION NAME AND ADDRESS
Naval Research Laboratory
Washington, D.C. 20375

10. PROGRAM ELEMENT, PROJECT, TASK AREA & WORK UNIT NUMBERS
NRL Problem G01-06
Project RR031-0341

11. CONTROLLING OFFICE NAME AND ADDRESS
NRL-8046

12. REPORT DATE
October 13, 1976

13. NUMBER OF PAGES
17

14. MONITORING AGENCY NAME & ADDRESS *(if different from Controlling Office)*
Office of Naval Research
Arlington, Va. 22217

15. SECURITY CLASS. *(of this report)*
Unclassified

15a. DECLASSIFICATION/DOWNGRADING SCHEDULE

16. DISTRIBUTION STATEMENT *(of this Report)*
RR031-03

Approved for public release; distribution unlimited

17. DISTRIBUTION STATEMENT *(of the abstract entered in Block 20, if different from Report)*
RR031-0341

18. SUPPLEMENTARY NOTES

19. KEY WORDS *(Continue on reverse side if necessary and identify by block number)*
Tornato, vortex, tornado skip, inertial oscillations, laboratory vortex, atmospheric vortex

20. ABSTRACT *(Continue on reverse side if necessary and identify by block number)*
Vortices generated in a rotating tank of water exhibited persistent oscillations which had periods close to the inertial period. The persistency of these oscillations suggested that tornado skip phenomen and the life cycle of concentrated atmospheric vortices might be closely linked with inertial oscillations of a tall vortex. This mechanism would provide a means to concentrate angular momentum near ground level to a larger extent than would steady inflow. Calculations of inertial periods for dust devils, water spouts, and tornadoes do agree with the skip interval for multiply occurring tornadoes or the life of concentrated atmospheric vortices.

DD FORM 1 JAN 73 1473 EDITION OF 1 NOV 65 IS OBSOLETE
S/N 0102-014-6601

SECURITY CLASSIFICATION OF THIS PAGE *(When Data Entered)*

CONTENTS

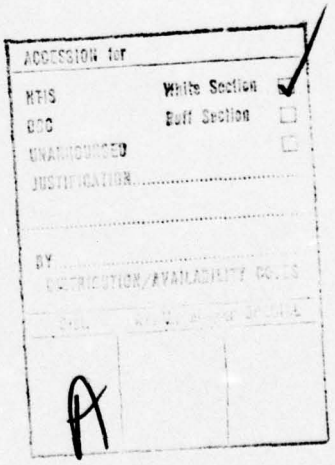

NONSTEADY LABORATORY SIMULATION OF ATMOSPHERIC VORTICES: INERTIAL OSCILLATIONS AND TORNADO SKIP

INTRODUCTION

It has been known for nearly a century [1] that a rotating column of fluid can exhibit a class of neutral modes called inertial oscillations. It is plausible to expect concentrated atmospheric vortices such as tornadoes, water spouts, and dust devils to exhibit inertial oscillations under proper conditions of forcing. As convection becomes established in a large cumulonimbus, surrounding low-level air is sucked into the base. This air will approximately conserve potential vorticity as it converges, thus causing the initiation of a concentrated vortex. As the convection accelerates, the rotating updraft may overshoot its equilibrium level more or less throughout the cell, causing a readjustment toward equilibrium in the form of a general downward motion of air in the cell. This situation would adjust to equilibrium through one or more damped inertial oscillations. The updraft portions of these oscillations have an accompanying strong horizontal convergence in the lower levels over and above that associated with the initial inflow, which in turn can produce the intense vortex observed as a tornado, water spout, or dust devil. As the updraft subsides and the downdraft sets in, a low-level outflow results which diverges angular momentum, thus causing the vortex to weaken. This mechanism would require that the life span of such a vortex should be closely related to the inertial period for it. In fact the inertial period should be a lower bound on the life cycle. In many cases tornadoes are observed to occur multiply from one long lived parent cell [2-4]. In this case the interval of occurrence of the tornadoes should be strongly controlled by the inertial period for the rotating system, if indeed such a situation is represented by a series of inertial oscillations.

The suggestion of a near-regular vortex oscillation was spurred on by some simple laboratory experiments in which a vortex was generated in a rotating tank of water. The vortex was always oscillatory, and during the updraft portion of the oscillation a strong concentration of angular momentum occurred at the base, as one would observe during tornado formation. The oscillation period was adequately given by the inertial oscillation period when the core was treated as a cylinder in solid rotation. This prompted the calculation of inertial periods for atmospheric vortices (combined Rankine vortices), with the result that the periods were generally a good lower bound on the life span of these vortices. In the case of multiple tornadoes their occurrence interval was somewhat longer than their inertial period. Thus it is felt that inertial oscillations of atmospheric vortices occur and exert a strong dynamical influence on the vortices when the external forcing is suitable.

Manuscript submitted August 10, 1976

Another major impetus for this report is that several investigators who have simulated laboratory vortices [5-7] have generally reported vortices which are steady or have rapid transitory perturbations. In this latter case no attempt has been made to identify the oscillatory phenomena. In the present experiments the oscillations could not be eliminated, no matter what precautions were taken to do so, which indicates they are an important feature of a vortex which is not directly coupled to the force which generates the updraft.

LABORATORY EXPERIMENTS

The vortices were simulated in a large Pyrex cylinder mounted on a variable-speed turntable (Fig. 1). Water was circulated through a pump and flowmeter and then upward from a nozzle in the center of the cylinder near the top. This water flowed directly out to the wall of the cylinder near the top, where it was removed with a manifold. The flow of water across the top induced a secondary flow across the top, down the sides, in across the bottom and finally up the vortex along the axis of the cylinder. The flow above the nozzle was turbulent for all the flow rates used. To make the flow visible, ink was injected just above the base of the cylinder and near the center.

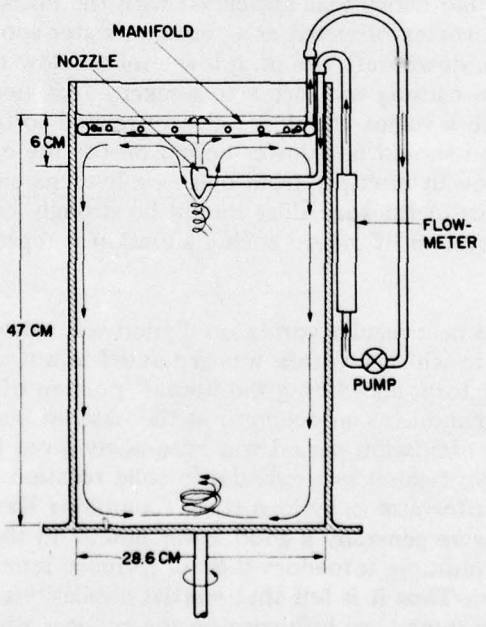

Fig. 1—Variable-speed rotating cylinder, the primary water-flow circuit, and the induced secondary flow which produces the central vortex

The quantities varied during the measurements were the flow rate through the nozzle Q and the rotation rate of the turntable Ω. For all combinations of Q (5 to 25 $cm^3\ s^{-1}$) and Ω (0.25 to 3.0 rad s^{-1}), a concentrated vortex was observed in the center of the cylinder. The vortex appeared to have a double structure—a concentrated core which had a large angular velocity ω_v and a wall about the core which rotated at a rate larger than Ω but less than ω_v. This structure is clearly evident in Fig. 2. The core is readily discernible at the top and near the bottom of the vortex. Both the core and the wall oscillate vertically, but the net flow is upward in both.

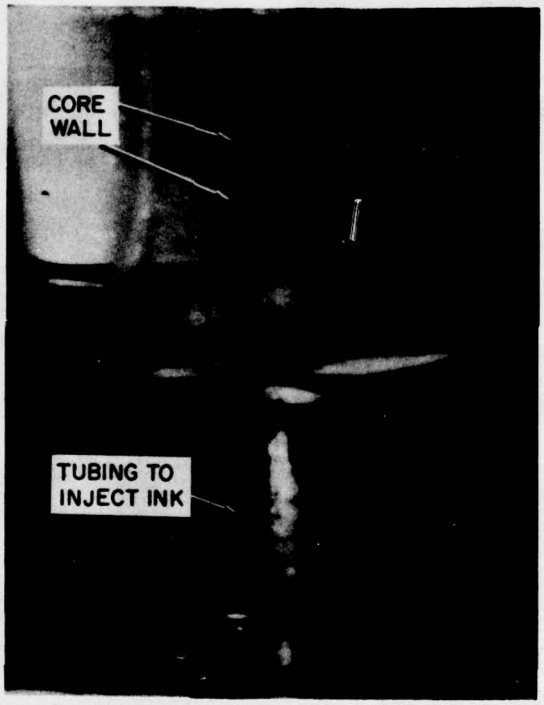

Fig. 2—Central core and outer wall of the vortex. The ink is injected from hypodermic tubing. Inflow to the vortex at the base has just been completed.

Typically the vortex was 3 cm in diameter, with some minor variation when Q and Ω were varied. For the range of variables used in the measuerments, ω_v varied from 1.5Ω at low Q up to 17.5Ω at the largest Q. There was only a weak dependence of ω_v/Ω on Ω.

In the vortex oscillation the center of the vortex moved up or down while the fluid immediately adjacent to the core moved in the opposite sense relative to the net upward flow in the vortex. A pure standing mode in the vertical was not observed. Generally there appeared to be a mixture of the first several modes occurring. A sequence of photos from a motion-picture record at Ω = 1.5 rad s^{-1} and Q = 15 $cm^3\ s^{-1}$ is given in Fig. 3;

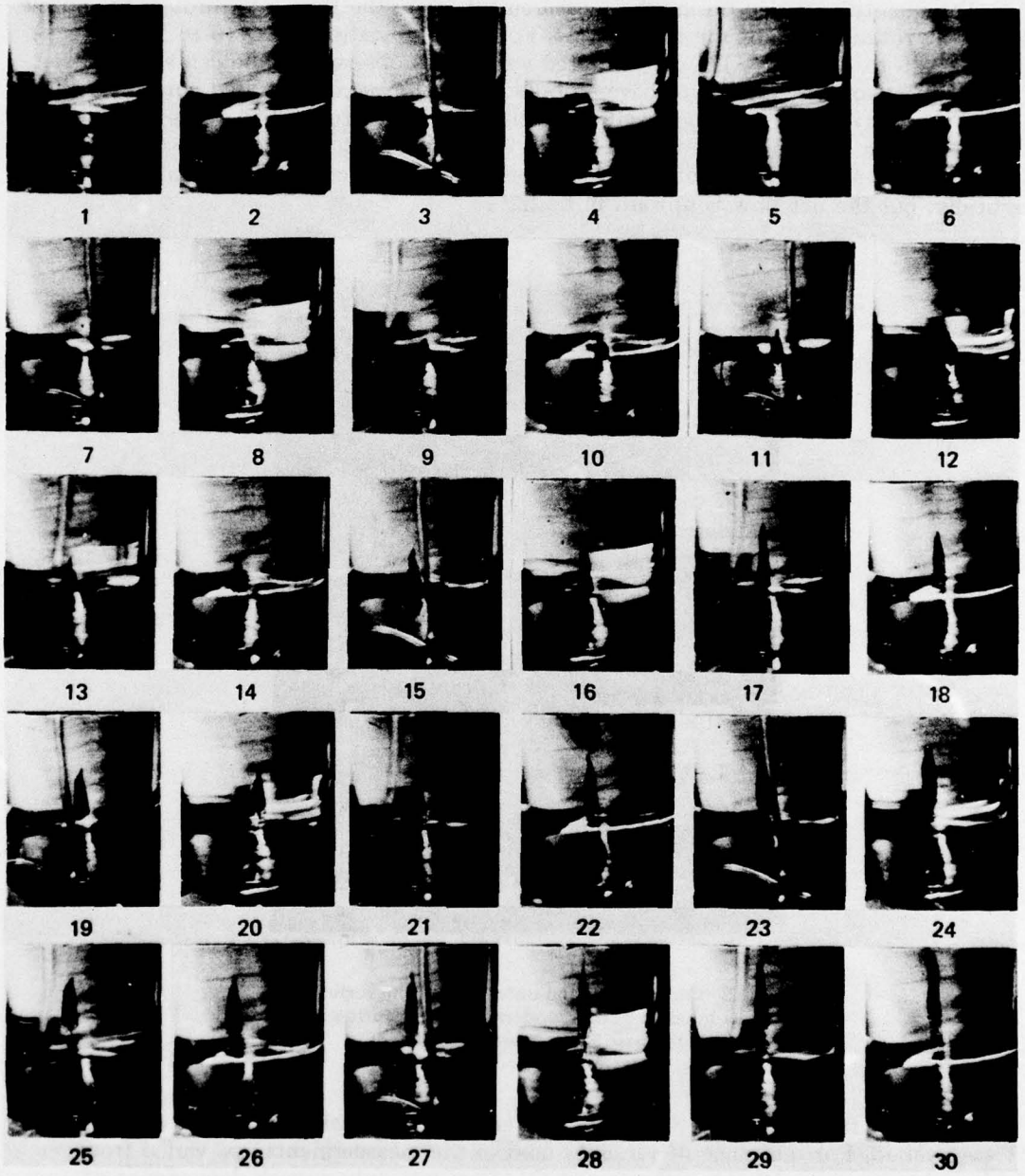

Fig. 3—Sequence showing the oscillations of the vortex. The core reaches the maximum vertical extent of oscillation at frames 4, 11, 17, and 23. The rotation rate of the apparatus is 1.5 rad s^{-1}, and each frame is 1/4 revolution (1.05 s) apart.

the frames are 1/4 revolution of the apparatus apart. The ink (the dark conical area which develops in the center) is injected about 2 mm above the base and about 2 vortex-core radii from the center of the cylinder. At frame 4 the core of the vortex has reached its maximum upward excursion and maximum ω_v. It then collapses downward through frame 6, and ω_v decreases markedly with the collapse. The core then rises until frame 11, collapses slightly and grows again until frame 17, when it collapses again. Another collapse occurs after frame 23. The double structure of the vortex is evident in frames 26 to 30.

The periods of these oscillations were measured over a fairly wide range of conditions. The periods are not highly regular, presumably due to the mixture of modes present, so averages were used in most cases. In Fig. 4 the angular frequency of the oscillation ω_{osc}, measured visually with a stopwatch, is plotted against the average rotataion rate of the vortex core, also measured visually with a stopwatch (and is compared with lines calculated using equations not yet discussed). The vertical bars show the range of frequencies observed.

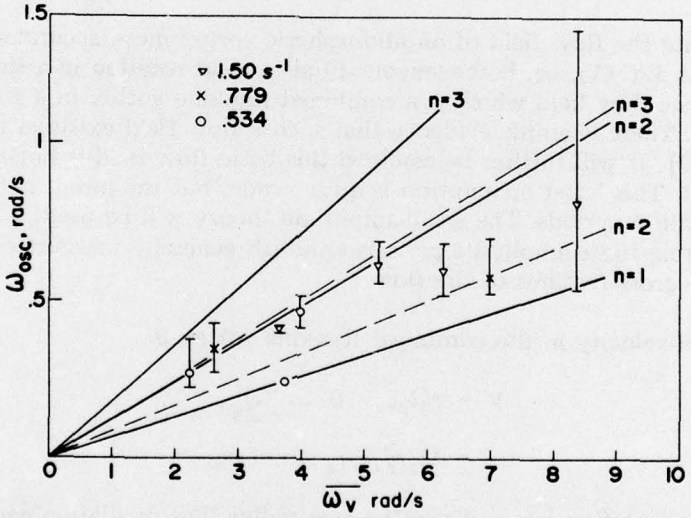

Fig. 4—Comparison of measured and calculated periods. The solid lines are from Eq. (1) and the dashed lines are from Eq. (3) for $\beta_0 = 2.405$. The range of measured points is due to the n irregularity of the oscillations.

The frequency ω_{osc} of a standing inertial mode having $n - 1$ nodal surfaces in the vertical (excluding the ends) in a cylinder of height d and radius r_0 in solid rotation is, according to Fultz [8],

$$\omega_0 = \frac{\omega_v}{\frac{1}{2}\sqrt{\left(\frac{\lambda_i d}{n\pi r_0}\right)^2 + 1}} \approx \omega_v \frac{2n\pi r_0}{\lambda_i d}, \qquad (1)$$

the latter being so when $\lambda_i d \gg n \lambda r_0$. Here λ_i is the ith root of $J_1(\lambda_i) = 0$ where J_1 is the ordinary Bessel function of the first order. For the present geometry the curves for $n = 1$, 2, and 3 ($\lambda_i = 3.833$) are drawn in Fig. 4 as the solid lines. The value of r_0 used is 1.5 cm, which was obtained from the photographs of Fig. 3, and d was taken as 39 cm, and "effective" depth. Typically the dominant n observed was 2 or 3. The measured frequencies, although somewhat irregular, do fall into the inertial range; hence it is concluded the observed oscillations are mixtures of several modes of inertial oscillations.

The source of the oscillations is obscure; however, since inertial oscillations are neutral, they will occur at or near their natural frequency when any forcing function is present which has components near the inertial frequencies. The small variations in the rotational drive, variations in the pump flow rate, and instabilities in the nozzle-manifold flow all contribute to the forcing. The important facts are: the fluid oscillations had the correct structure and roughly the proper periods so they could only be inertial oscillations.

THEORY

To approximate the flow field of an atmospheric vortex more accurately than the theory which led to Eq. (1), i.e. homogeneous fluid in solid rotation in a finite cylindrical container, a basic flow field which is a combined Rankine vortex in a stratified atmosphere will be used. There is ample evidence that such a flow field exists in tornadoes [9] and dust devils [10]. It will further be assumed this basic flow field is horizontal and height independent. This latter assumption is quite crude, but the intent here is to obtain approximate oscillation periods. The small-amplitude theory will be used; it is quite reliable for estimating finite-amplitude periods although generally inaccurate in specifying any more than the gross features of the flow.

The tangential velocity in the combined Rankine vortex is

$$V = r\Omega_c, \quad 0 < r < r_c, \tag{2a}$$

$$= \Omega_c r_c^2 / r, \; r_c < r < \infty, \tag{2b}$$

where Ω_c is the core rotation rate and r_c is the core radius. The oscillation period is then (the details are left to Appendix A)

$$\tau = \frac{\pi \beta_0}{V_T \gamma}, \tag{3}$$

where

$$V_T = r_c \Omega_c, \; J_0(\beta_0) = 0,$$

and

$$\gamma^2 = \frac{\pi^2}{H^2} + \frac{a^2}{4}, \tag{4}$$

in which H is the height of the tornado vortex and a^{-1} is the equivalent depth of the atmosphere when the density is given by $\rho = \rho_0 e^{-az}$ ($a^{-1} = 9.5 \times 10^3$ m).

It is assumed for (3) that $\gamma \ll 1$, $\beta_0^2 \ll \gamma^2 r_c^2$, and $aV_T^2/g \ll 1$. For $V_T = 100$ m s^{-1} this term is 0.1, and this value is approached only for large or intense tornadoes. This result is similar to (1), except here the roots of J_0 and the factor γ^{-1} enter.

The vertical velocity field, obtained from (A4) and (A9), is

$$w = \frac{\beta_0}{r_c} A J_0\left(\frac{\beta_0 r}{r_c}\right) e^{az/2} \sin\frac{\pi z}{H} \cos\sigma t, \qquad 0 < r < r_c, \tag{5a}$$

$$= \gamma A \frac{J_1(\beta_0)}{K_1(\gamma r_c)} K_0(\gamma r) e^{az/2} \sin\frac{\pi z}{H} \cos\sigma t, \qquad r_c < r < \infty . \tag{5b}$$

COMPARISON WITH OBSERVATIONS

The explicit value of β_0 has not been chosen as yet. The experiments showed two distinct regions of vertical motion in the vortex, but it was not clear if they were sometimes opposite in direction because of the net vertical flow superimposed on the vortex. A similar double structure was observed by Sinclair [10] in dust devils. Sinclair's data shows a definite reversal in w. From (5) this occurs when β_0 is chosen as the second zero of $J_0(\beta_0 = 5.507)$. Some tornadoes, such as the Dallas tornado, show a strong tendency toward a first-mode structure. Then $\beta_0 = 2.405$.

According to (3) the period of the oscillation requires a knowledge of V_T and H (since γ is a function of H). We are assuming τ represents either the duration of the phenomena or the occurrence interval in the case of successive multiple tornadoes being spawned from the same parent cloud. Until recently data on V_T and H were almost impossible to obtain. Burgess, Lemon, and Brown [11] have recently obtained doppler radar data from a tornado which touched down at Union City, Oklahoma, and produced intense damage. They found a region of intense shear in the cloud with an average maximum tangential velocity of 27 m s^{-1} at 0.2-km and 3.5-km elevations. They state that this intense shear zone (presumably the tornado vortex) extended to 10 km and retained vertical continuity through this range. The cloudtops on radar were at a height of 15 km. The strong shear region observed near the ground level definitely corresponded with the observed tornado position. This confirms that a tornado is a continuous vortex extending vertically through most of the cloud mass.

The tangential velocities observed in the cloud are much less than those which produced "intense damage" at ground level (which are denoted $v_{\max,\, d}$). Based on Ref. 4, considerable damage occurs for winds of 50 to 70 m s^{-1} ($F2$ winds), and severe damage occurs for winds of 70 to 90 m s^{-1} ($F3$ winds). The Union City tornado had a translational speed v' of 8 knots, so the "damage" tangential velocity ($v_{\max,\, d} - v'$) was 62 to 82 m s^{-1}, or 1.5 to 3 times the tangential velocity observed in the cloud.

Also, if (3) is used to estimate periods, V_T represents an average tangential velocity, whereas the velocity observed by Burgess, Lemon, and Brown [11] would be a maximum value v_{max}, because this is when the vortex reaches sufficient intensity to manifest itself. If we let α represent the amplitude of the inertial oscillation as a fraction of the basic state, then

$$1 + \alpha = v_{max}/V_T. \tag{6}$$

Also, if s represents the ratio of the damage tangential velocity ($v_{max,\,d} - v'$) to v_{max}, then (3) becomes

$$\tau = \frac{\pi\beta_0(1+\alpha)}{V_{max}} \tag{7}$$

or

$$\tau = \frac{\pi\beta_0 s(1+\alpha)}{V_{max,\,d} - v'}. \tag{8}$$

The Union City tornado suggests $s \approx 2$. The amplitude α is uncertain, but a range of 0.2 to 0.5 is reasonable. The basic state velocity V_T for our theory should be the tangential velocity of the parent rotating updraft. This is obtained here through the factors α and s.

Data for several documented tornado occurrences (Dallas [4, 9], Fargo and Palm Sunday [9], and Union City [11]) along with dust-devil data [10] and waterspout data [Golden, private communication] are used for comparison. For the Fargo and Palm Sunday occurrences $v_{max,\,d}$ is available. For Dallas the largest velocities Hoecker [9] gives are from 30 m to about 250 m above the ground and are 75 m s^{-1}. The damage estimates from Dallas give velocities ranging from 45 to 80 m s^{-1}. The cloudtop height is used for H. For Dallas the tropopause height was used, and for the Palm Sunday tornadoes 15 km was arbitrarily chosen. The occurrence interval for the tornadoes is taken from Fujita [4]. For the Fargo and Palm Sunday tornadoes Eq. (8) was used, and for the other cases Eq. (7) was used.

The values of τ for $\alpha = 0.2$ and 0.5 are given in Table 1. These calculated periods are also plotted against the observed periods in Fig. 5, differentiated by mode and whether a duration or interval of occurrence was given. The inertial period is more closely related to the interval than to the duration; however the duration should be a significant fraction of the period, depending on the swirl intensity of the parent storm. In any case the duration should be bounded above by the inertial period.

CONCLUDING REMARKS

This calculation of the inertial period neglects many factors, the most important of which are nonlinear effects and interactions of the vortex with the ground. It is intended to show, within a factor of 2 over a period range of two decades, that inertial periods agree with natural vortex lifetimes or occurrence intervals and that the presence of an

Table 1 — Vortex Quantities

Event	Occurrence Interval (s)	Duration (s)	$\tau(s)$				Vortex Quantities				
			Mode 1		Mode 2		V_{max} (m s^{-1})	$V_{max,\,d}$ (m s^{-1})	v' (m s^{-1})	r_0 (m)	H (km)
			$\alpha = 0.2$	$\alpha = 0.5$	$\alpha = 0.2$	$\alpha \approx 0.5$					
Union City	-	1500	863	1079	1976	2471	33	-	8	-	10.0
Dallas	1620	2100	603	755	1383	1728	73	45-80	12	55	13.1
Fargo	2640	-	1394	1743	3193	4005	-	82	9	320	18.4
Palm Sunday	2880	-	1622	2027	3736	4640	-	80	28	165	15.0
Waterspout	-	480-720	410	513	941	1176	35	-	-	25	0.5
Dust devil	-	60-240	86	108	226	282	10	-	-	6	0.3

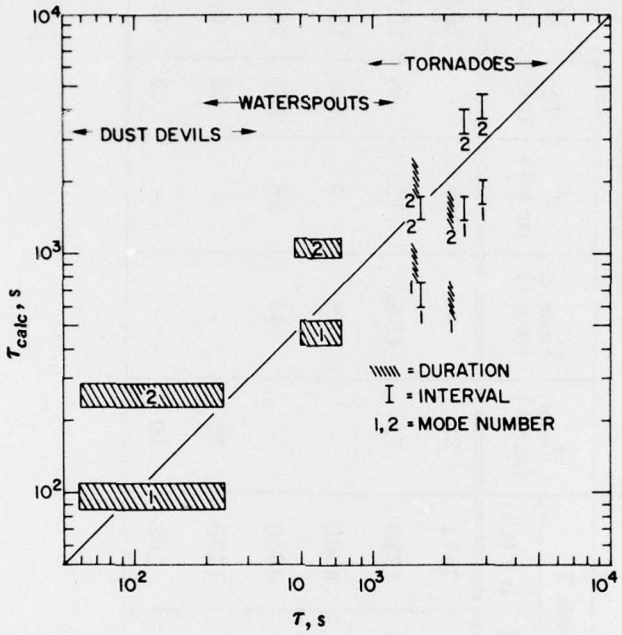

Fig. 5—Comparison of calculated and observed periods for dust devils, waterspouts, and tornadoes. Data for the duration of the vortex and for the interval between occurrences are given. Both modes are included.

inertial oscillation on a vortex should be expected when variable natural forcing is present. The inertial oscillation provides a mechanism whereby angular momentum can be concentrated into an intense vortex. The use of a linear theory here is an approximate treatment of the problem. Numerical or other nonlinear time-dependent calculations should provide more accurate estimates of intervals or durations, if inertia oscillations are the fundamental mechanism controlling atmospheric vortex formation.

ACKNOWLEDGMENTS

The measurements that have been analyzed in this report were done in the Hydrodynamics Laboratory of the University of Chicago under National Science Foundation grant NSF GS-28689 and National Aeronautics and Space Administration grant NGR-14-001-008.

REFERENCES

1. Lord Kelvin, "Vibrations of a Columnar Vortex," *Phil. Mag.* **10,** 155-168 (1880).
2. G.L. Darkow, and J.C. Roos, 1970. Multiple tornado producing thunderstorms and their apparent cyclic variations in intensity. *Preprint Volume - 14th Radar Meteor. Conf.*, Meteor. Soc., Boston, Mass. 305-308.
3. G.L. Darkow, 1971. Periodic tornado production by long-lived parent thunderstorms. *Preprint Volume - Seventh Conf. on Severe Local Storms,* Amer. Meteor. Soc., Boston, Mass., 214-217.
4. T. Fujita, 1971. Proposed characterization of tornadoes and hurricanes by area and intensity. Satellite and Mesometeorology Research Project Res. Paper No. 91, University of Chicago, Chicago, Ill.
5. N.B. Ward, 1972. The exploration of certain features of tornado dynamics using a laboratory model, *J. Atmos. Sci.*, **29,** 1194-1204.
6. C.A. Wan, and C.C. Chang, 1972. Measurement of the velocity field in a simulated tornado-like vortex using a three-dimensional velocity probe, *J. Atmos. Sci.*, **29,** 116-127.
7. D.E. Fitzjarrald, 1973. A laboratory simulation of convective vortices. *J. Atmos. Sci.*, **30,** 894-902.
8. D. Fultz, 1959. A note on overstability and the elastoid-inertial oscillations of Kelvin, Solberg, and Bjerknes, *J. Meteor.*, **16,** 199-208.
9. W.H. Hoecker, 1960. Wind speed and air flow patterns in the Dallas tornado of April 2, 1957, *Mon. Wea. Rev.*, **88,** 167-180.
10. P.C. Sinclair, 1973. The lower structure of dust devils, *J. Atmos. Sci.*, **30,** 1599-1619.
11. D.W. Burgess, L.R. Lemon, and R.A. Brown, "Tornado Characteristics Revealed by Doppler Radar," *Geophys. Res. Letters* **2,** 183-184 (1975).

Appendix A

DERIVATION OF EQ. (3)

Consider a cylindrical coordinate system in which r, θ, and z are respectively the radial, tangential, and vertical coordinates. The oscillation velocity components in the r, θ, and z directions respectively are u, v, and w. Then the appropriate linearized equations of motion for axisymmetric motion, with a basic axisymmetric velocity $V = V(r)$, are

$$\rho\left(\frac{\partial u}{\partial t} - 2V\frac{v}{r}\right) = -\frac{\partial p}{\partial r}, \tag{A1a}$$

$$\rho\left(\frac{\partial v}{\partial t} + u\frac{\partial V}{\partial r} + V\frac{u}{r}\right) = 0, \tag{A1b}$$

$$\rho\left(\frac{\partial w}{\partial t}\right) = -\frac{\partial p}{\partial z}, \tag{A1c}$$

and

$$\frac{\partial u}{\partial r} + \frac{u}{r} + \frac{\partial w}{\partial z} = 0 \tag{A1d}$$

with

$$-\rho\frac{V^2}{r} = \frac{\partial P}{\partial r} \tag{A1e}$$

and

$$0 = -\frac{\partial P}{\partial z} - g\rho, \tag{A1f}$$

where P is the pressure distribution for the basic state, p is the perturbation pressure, and g is gravity. Since the atmosphere is stratified, let

$$\rho = \rho_0(r)e^{-az}, \tag{A2}$$

where $a^{-1} = 9.5 \times 10^3$ m. From (A1e) and (A1f)

$$\frac{1}{\rho_0}\frac{d\rho_0}{dr} = \frac{aV^2}{rg}. \tag{A3}$$

Introduce a Stokes' stream function ψ as

$$u = -\frac{1}{r}\frac{\partial \psi}{\partial z}, \tag{A4a}$$

and

$$w = \frac{1}{r}\frac{\partial \psi}{\partial r}, \tag{A4b}$$

so (A1) becomes upon elimination of u, v, w and retention of the r and z density variations

$$\frac{\partial^2}{\partial t^2}\left[\frac{aV^2}{r^2 g}\frac{\partial \psi}{\partial r} + \frac{\partial}{\partial r}\left(\frac{1}{r}\frac{\partial \psi}{\partial r}\right)\right] + \left(\frac{\partial}{\partial z} - a\right)\left[\frac{\partial^2}{\partial t^2} - \frac{2V}{r}\left(\frac{V}{r} + \frac{\partial V}{\partial r}\right)\right]\frac{1}{r}\frac{\partial \psi}{\partial z} = 0. \tag{A5}$$

The solution is of the form

$$\psi = \psi'(r)(\cos \sigma t)e^{az/2}\sin\frac{\pi z}{H}, \tag{A6}$$

where σ is a constant to be determined and H is the total height of the vortex. Substitution of (A6) into (A5) yields

$$\frac{\partial^2 \psi'}{\partial r^2} + \left(\frac{aV^2}{g} - 1\right)\frac{1}{r}\frac{d\psi'}{dr} + \left[\frac{2V}{r\sigma^2}\left(\frac{V}{r} + \frac{\partial V}{\partial r}\right) - 1\right]\gamma^2 \psi' = 0, \tag{A7}$$

in which

$$\gamma^2 = \frac{\pi^2}{H^2} + \frac{a^2}{4}. \tag{A7}$$

The combined Rankine vortex is described by

$$V = r\Omega_c, \quad 0 \leqslant r \leqslant r_c \qquad \text{(inner region, I)}, \tag{A8a}$$

$$= r_c^2 \Omega_c / r, \quad r_c \leqslant r \leqslant \infty \qquad \text{(outer region, O)}. \tag{A8b}$$

In both regions (A7) has solutions in closed form when $aV^2/g = 0$. For the most intense tornadoes $V \leqslant 100$ m s^{-1}; hence

$$\frac{aV^2}{g} < 10^{-1},$$

and this term can be neglected in comparison to unity. Then the solutions for the inner and the outer regions are respectively

$$\psi_I = A_I(\cos \sigma t)e^{az/2}\left(\sin \frac{\pi z}{H}\right) rJ_1(\beta r),\ 0 < r \leqslant r_c, \tag{A9a}$$

$$\psi_O = A_O(\cos \sigma t)e^{az/2}\left(\sin \frac{\pi z}{H}\right) rK_1(\gamma r),\ r_c \leqslant r < \infty, \tag{A9b}$$

where J_1 is the ordinary Bessel function of the first order, K_1 is the modified Bessel function of the first order, and

$$\left(1 - \frac{4\Omega_c^2}{\sigma^2}\right)\gamma^2 + \beta^2 = 0. \tag{A10}$$

To determine β and A_I in terms of A_O, the solutions are matched at r_c:

$$\psi_I(r_c) = \psi_O(r_c) \tag{A11a}$$

and

$$\left.\frac{\partial \psi_I}{\partial r}\right|_{r_c} = \left.\frac{\partial \psi_O}{\partial r}\right|_{r_c} \tag{A11b}$$

This gives

$$A_I = A_O K_1(\gamma r_c)/J_1(\beta r_c) \tag{A12}$$

and

$$\beta J_0(\beta r_c)/J_1(\beta r_c) = \gamma K_0(\gamma r_c)/K_1(\gamma r_c).$$

Typically for a small tornado, r_c = 100 m and $H = 10^4$ m [11], giving $\gamma = 3 \times 10^{-4}$ m^{-1}; hence to a high degree of approximation

$$\beta J_0(\beta r_c) \approx 10^{-5} J_1(\beta r_c) \approx 0 \tag{A13a}$$

and

$$\beta = \beta_0/r_c, \tag{A13b}$$

where

$$J_0(\beta_0) = 0.$$

Then from (A6) the oscillation period τ is

$$\tau = \frac{2\pi}{\sigma} = \frac{\pi}{\Omega_c}\left(1 + \frac{\beta_0^2}{\gamma^2 r_c^2}\right)^{1/2} \tag{A14}$$

or, since $\beta_0^2/r_c^2 \gg \gamma^2$,

$$\tau = \frac{\pi\beta_0}{V_T\gamma},$$

where

$$V_T = r_c\Omega_c. \tag{A15}$$